CrystEngComm

PAPER

View Article Online
View Journal

Cite this: DOI: 10.1039/c8ce01757c

Substituent effects in solid-state assembly of activated benzotriazoles†

Daniel S. Wenholz,[a] Mohan Bhadbhade,[b] Hakan Kandemir,[ac] Junming Ho,[a] Naresh Kumar [a] and David StC. Black *[a]

Received 15th October 2018,
Accepted 19th December 2018

DOI: 10.1039/c8ce01757c

rsc.li/crystengcomm

Aromatic donor–acceptor stacking involving electron-rich π-donors and electron-deficient π-acceptors has been utilized in a broad spectrum of diverse applications to great effect. We report the discovery of unprecedented donor–acceptor stacking from a non-mixed activated benzotriazole scaffold to give cofacial π-stacking in 2D sheets. We further report the effects of altering the substituents of the bicyclic aromatic system. It was found that any alteration made to the substituents disrupted the cofacial stacking, however, both aromatic donor–acceptor stacking and 2D sheet formation was observed in the solid-state assembly of the analogues. Furthermore, interactions that satisfied both electrostatic and direct-substituent π-stacking models were observed.

Introduction

Noncovalent aromatic interactions such as π-stacking play fundamental roles within supramolecular chemistry and biological recognition.[1,2] These interactions are of key importance in both synthetic applications, such as self-assembly architectures,[3] to naturally occurring phenomena including DNA base–base interactions.[4–6] Despite this prominence, π-interactions remain perhaps the least understood noncovalent interaction.

In the 1990s a model explanation was postulated by Hunter and Sanders in which electrostatics brought about by the quadrupole moment of each ring play a dominant role in π–π interactions. This "electrostatic model" was used to explain a perceived preference for electron deficient aromatic systems to stack with electron rich aromatics in a face-centered manner.[7] By this explanation, the main attractive force was due to the differential polarization between the two aromatic systems.[8] The resultant alternated stacking between electron rich and electron deficient aromatics has since been referred to as "aromatic donor–acceptor" stacking or interactions.[9] More recent experimental work by Rashkin and Waters[10] and Snyder *et al.*,[11] along with numerous computational studies,[12–16] have shown that direct substituent–substituent and substituent–ring interactions play a major role in the degree of cofacial overlap of stacked ring systems. However, there has been limited discussion on how this "direct interaction model" applies to aromatic donor–acceptor stacking.

Since their inception donor–acceptor interactions have been utilized to great effect in molecular architectures,[17–21] self-assembly,[22–26] self-healing polymers,[27,28] molecular recognition[29–32] and catalysis.[33] Stoddart and co-workers have used a variety of aromatic donor–acceptor systems in the self-assembly of molecular architectures of catenanes and rotaxanes.[34–39] These works have included the use of electron deficient bipyridinium residues as π-acceptors and electron rich 1,5-dialkoxynaphthalene (DAN), hydroquinone, and resorcinol residues as π-donors. Iverson and co-workers have undertaken extensive work on DAN donor and 1,4,5,8-

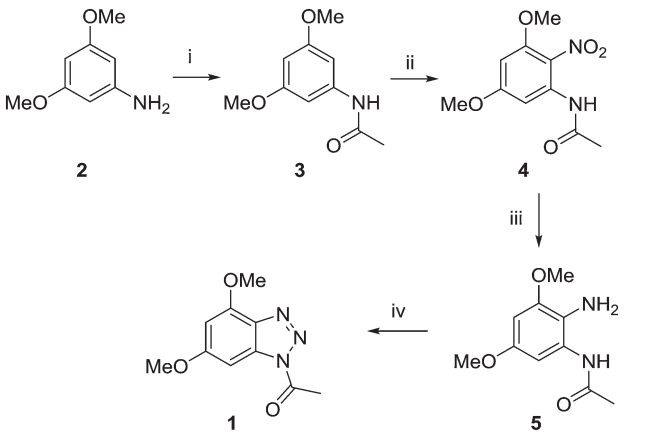

Scheme 1 Reagents and conditions; i) Ac_2O, 0 °C, 2 h, 94%; ii) HNO_3/Ac_2O, 0 °C, 30 min, 59%; iii) $N_2H_4{\cdot}H_2O$, Pd/C, EtOH, reflux, 2 h, 98%; iv) $NaNO_2$/HCl, 0 °C, 10 min, 87%.

[a] School of Chemistry, UNSW Sydney, Australia. E-mail: d.black@unsw.edu.au
[b] Mark Wainwright Analytical Centre, UNSW Sydney, Australia
[c] Department of Chemistry, Faculty of Art and Science, Namik Kemal University, Tekirag, Turkey

† Electronic supplementary information (ESI) available: Experimental procedures, characterisation data, and X-ray crystal data. CCDC 1856989–1856995. For ESI and crystallographic data in CIF or other electronic format see DOI: 10.1039/c8ce01757c

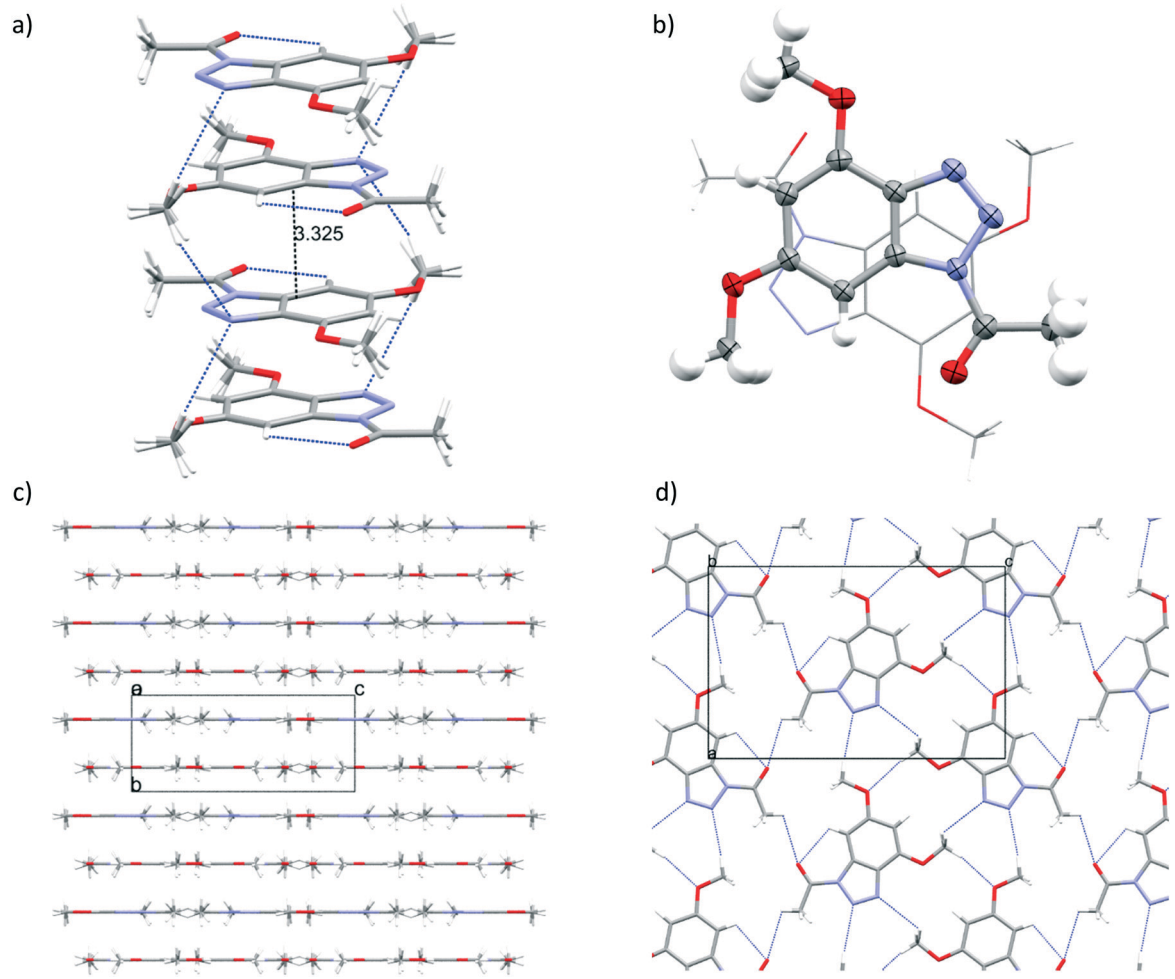

Fig. 1 X-ray crystal structure of activated benzotriazole **1** with hydrogen bonds displayed as blue dotted lines; a) anti-parallel continuous stacking with perpendicular stacking distance displayed as black dotted line, distance measured in angstroms; b) overlap of ring systems as viewed along *b*-axis, ellipsoids are shown at 50% probability; c) 2D sheets viewed along *a*-axis; d) single layer of 2D sheets viewed along *b*-axis.

naphthalenetetracarboxylic diimide (NDI) acceptor systems in numerous applications including foldamers,[40] the self-assembly of aggregates[41] and macromolecules,[42] artificial DNA bases,[43] thermochromic materials,[44] and mesophases.[45]

Although reports of a limited number of DAN–NDI and related donor–acceptor system cocrystals exist in the literature,[20,21,31,44–46] there is a distinct lack of crystal structures exhibiting donor–acceptor stacking from a homo-molecular or non-mixed system. Whilst such homo-molecular interactions have been observed in dyads developed for organic-based devices, these typically involve very large aromatic polycycles including perylenes and hexabenzocoronenes.[47,48] Based upon the DAN–NDI system, Peebles *et al.* developed a series of significantly smaller donor–acceptor dyads consisting of covalently linked mono-alkoxynaphthalene (MAN) and naphthalimide (NI) units.[49] Whilst non-continuous face-to-face donor–acceptor interactions were observed between neighbouring molecules in some dyad crystal structures, the only evidence for continuous alternating donor–acceptor stacking came from powder XRD analysis of dyad crystals grown from fast evaporating solvent. Crystal structures for similar MAN–NI dyads developed by Benanti *et al.* showed only donor–donor and acceptor–acceptor stacking, although it should be noted that this stacking is beneficial to an organic-based device.[50]

The formation of cofacial π-stacked aromatic ring systems in 2D sheets has been sought after to improve charge-carrier transport efficiency due to increased overlap in molecular orbitals.[51,52] In this study we report the rather serendipitous discovery of homo-molecular stacking from substituted benzotriazoles possessing both π-donor and π-acceptor moieties and its use to study substituent effects on aromatic stacking.

Results and discussion

Activated benzotriazole **1** was originally developed as an electron rich reagent similar to other activated heterocycles made previously by our group.[53,54] It was prepared by first protecting 3,5-dimethoxyaniline **2** with acetic anhydride at 0 °C, followed by nitration of acetamide **3** with nitric acid in acetic anhydride to give 2-nitro-3,5-dimethoxyacetamide **4**.

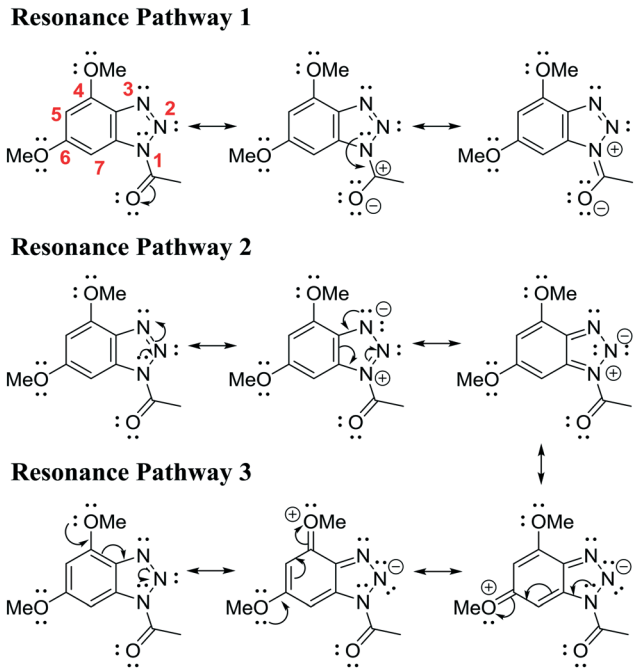

Fig. 2 Electronic resonance pathways of activated benzotriazole **1**.

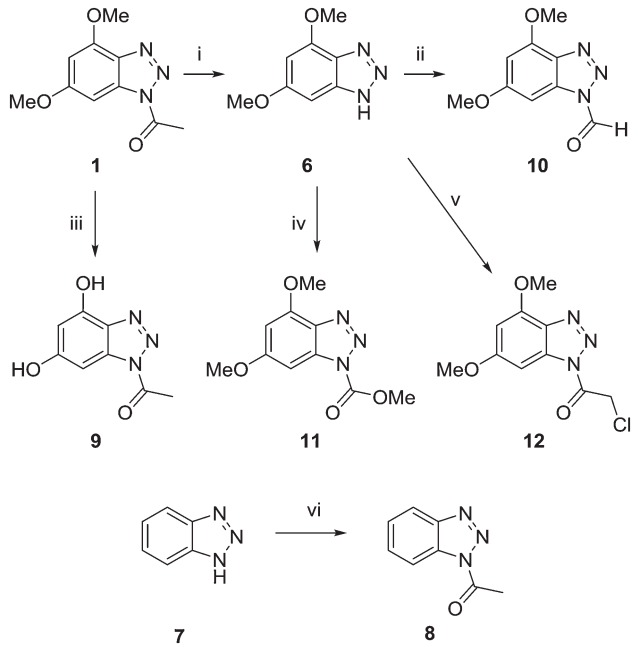

Scheme 2 Reagents and conditions; i) KOH, MeOH, rt, 30 min, then 10% H_3PO_4, 86%; ii) acetic formyl anhydride, −5 °C, 1 h, 66%; iii) $AlCl_3$, PhMe, 150 °C, 1.5 h, 31%; iv) BTC, Et_3N, THF, rt, 1 h, then MeOH, 65%; v) chloroacetyl chloride, K_2CO_3, acetone, 0 °C then rt, 3 h, 86%; vi) acetyl chloride, Et_3N, DCM, 0 °C, 30 min, 78%.

Palladium-catalysed hydrazine reduction of the introduced nitro group yielded 2-acetamidoaniline **5**, which was subsequently diazotized and cyclised in one step to the novel substituted *N*-acetylbenzotriazole **1** by treatment with sodium nitrite in cooled hydrochloric acid (Scheme 1).

Originally developed solely for structure confirmation, the single crystal structure of activated benzotriazole **1** showed an unexpectedly remarkable stacking structure. Most noticeably, the crystal structure showed a continuous anti-parallel head-to-tail stacking of benzotriazole molecules, resulting in heterogeneous cofacial π-stacking between the benzene and triazole rings of neighbouring molecules with considerable overlap (Fig. 1a and b). Our interest was even further aroused when we observed that the molecules had also arranged into perfectly flat 2D sheets to form a network of coplanar weak carbon–hydrogen bonds (Fig. 1c and d). In addition to these atypical features, the interplanar stacking distance was measured to be considerably short at 3.325 ± 0.001 Å.[7,55]

We were keenly interested to understand the underlying phenomena behind this curious crystal structure. A search of compounds with a benzo[1,2,3]triazole nucleus in the Cambridge Crystallographic Data Centre (CCDC) showed that out of over 500 such compounds only two exhibited both continuous anti-parallel cofacial stacking and formation of 2D sheets.[56,57] Whilst this demonstrated the rarity of this type of solid state assembly, it was notable that both database structures possessed a cationic charge at N3. Therefore, the head-to-tail interaction in these structures was likely influenced by favorable π–cation interactions. Although activated benzotriazole **1** lacked any such charge, we speculated that its triazole ring was likewise preferentially stacking with the benzene due to an attractive electrostatic interaction.

The preference for the methoxy-substituted ring to overlap with the acyl-substituted ring bore a striking resemblance to the aromatic donor–acceptor DAN–NDI electrostatic attraction interaction. We reasoned that orbitals of N1 of activated benzotriazole **1** were immensely electron-deficient from a combination of electron withdrawing effects of its acetyl substitution and resonance associated with the permanent dipole of N2 and N3, as shown in Fig. 2 (resonance pathways 1 and 2, respectively).[58] Although electron-deficient N1 was covalently bound to the electron rich benzene ring, its *meta*-positioning to the electron donating methoxy groups meant that the donated electrons were instead channelled to N2 and N3 (resonance pathway 3). Furthermore, the adjacent acyl α-carbon would likewise be electron deficient due to the inductive effect of the carbonyl oxygen (resonance pathway 1).

We therefore hypothesised that the association of this electron-deficient portion of the 5-membered ring with the comparatively electron-rich 6-membered benzene was due to electrostatic attraction. Although this reasoning for an aromatic–aromatic interaction largely followed Hunter and Sanders' electrostatic model, a short contact between the electron-rich benzene ring and electron-deficient acetyl α-carbon indicated that the substituent was also involved in the π interaction. This substituent–aromatic interaction was more in line with the direct interaction model, however, it could not be said which was the more influential factor. A very similar substituent–aromatic interaction can be observed in the majority of the previously mentioned donor–acceptor co-crystals, where the electron-rich naphthalene ring significantly overlaps the non-aromatic imide substituent ring.[20,21,31,45,46]

Table 1 Crystal structure packing details

Compound	N1 substituent	4,6-Substitution	Continuous π–π stacking	Alignment	Packing mode	Interplanar distance[c] (Å)
1	$COCH_3$	OMe	Yes[a]	Anti-parallel	Cofacial	3.325 ± 0.001
6	H	OMe	No[a]	Anti-parallel	Brick layer	3.373 ± 0.004 (3.410 ± 0.002)
8	$COCH_3$	H	Yes	Parallel	Herringbone	3.326 ± 0.001
9	$COCH_3$	OH	Yes[a,b]	Anti-parallel	Slipped	3.324 ± 0.003 (3.212 ± 0.002)
10	CHO	OMe	Yes	Parallel	Herringbone	3.252 ± 0.004
11	COOMe	OMe	Yes	Parallel	Herringbone	3.257 ± 0.003
12	$COCH_2Cl$	OMe	Yes	Parallel	Herringbone	3.368 ± 0.009

[a] 2D sheet formation. [b] Asymmetric π-stacking. [c] Measurement uncertainties listed as estimated standard deviations.

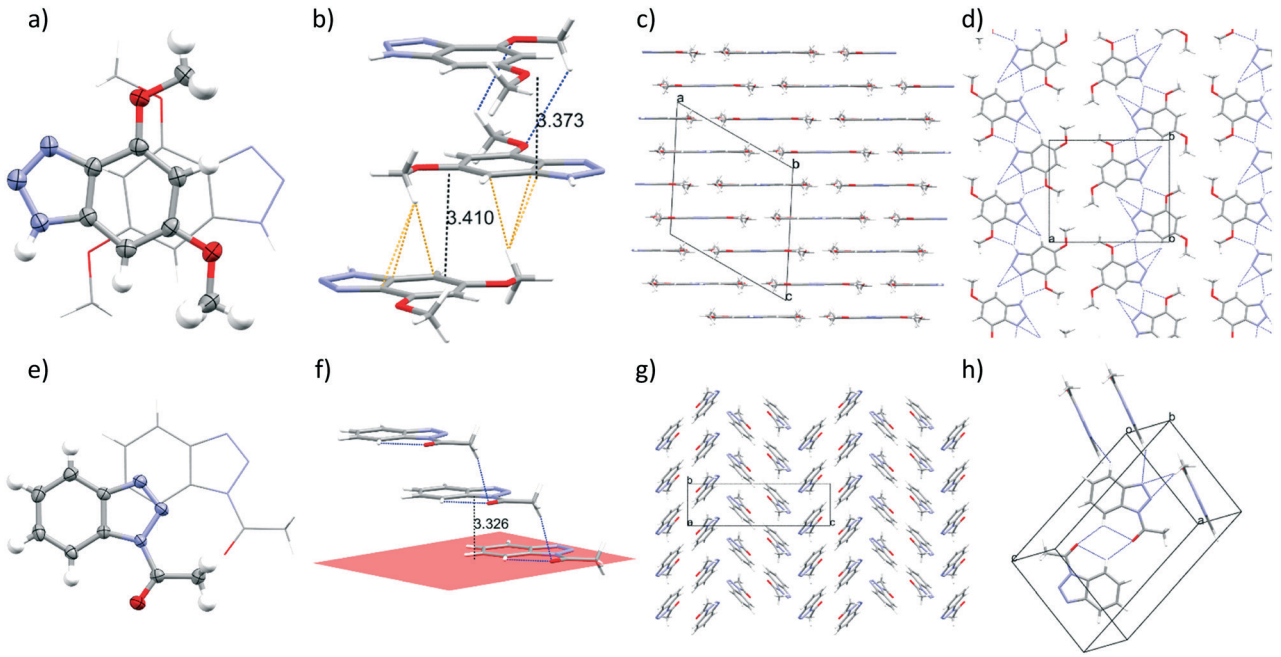

Fig. 3 X-ray crystal structures of parent benzotriazole **6** (a–d) and unactivated benzotriazole **8** (e–h), ellipsoids are shown at 50% probability, hydrogen bonds, CH–π short contacts and perpendicular stacking distances are displayed as blue, orange and black dotted lines, respectively, all distances measured in angstroms; a) stacking interaction viewed along *c*-axis; b) side view of non-continuous stacking and interplanar distance; c) 2D sheets viewed along *b*-axis; d) single layer of 2D sheets viewed along *c*-axis; e) ring-overlap of continuous stacking; f) side-view of parallel continuous stacking; g) herringbone array viewed along *b*-axis; h) co-planar hydrogen bonding.

The ring overlap in the stacking interaction of activated benzotriazole **1** appeared to be further stabilized by a carbon–hydrogen bond between the 6-methoxy substituent and N3 of the neighbouring molecule (Fig. 1a).

Whilst it was clear that the ring substituents were playing roles in the alternated stacking, it was unclear if they played any major role in the formation of the perfectly flat 2D sheets. We therefore set out to not only determine if the cofacial stacking could be influenced by altering the electron withdrawing/donating character of the substituents, but also whether any changes to the scaffold would affect 2D sheet formation.

The simplest way to examine if the substituents were playing a role was their removal from the scaffold. Likewise, the degree to which the 6-methoxy to N3 carbon–hydrogen bond contributed to ring overlap could be determined by demethylating the substituent so that it lacked the capability to form the interaction. Lastly, by varying the electron withdrawing ability of the N1 substituent, changes in the stacking interactions could be observed with varying electrostatic landscapes of the analogues.

The *N*-acetyl group from benzotriazole **1** was easily removed using potassium hydroxide in methanol followed by acidification with 10% phosphoric acid, yielding the parent 4,5-dimethoxybenzotriazole **6** in good yield. Benzotriazole **7** was treated with acetyl chloride to obtain the unsubstituted *N*-acetylbenzotriazole **8**. Demethylation of the methoxy groups of benzotriazole **1** was achieved by treatment with aluminium chloride, yielding *N*-acetyl-4,6-dihydroxybenzotriazole **9**.

Parent 4,5-dimethoxybenzotriazole **6** allowed easy access to changes in substitution at N1 with groups of varying electron withdrawing character. Firstly, parent benzotriazole **6** was reacted with acetic formic anhydride, which was formed immediately prior from acetic anhydride and formic acid. Following observations from Pasqua *et al.*,[59] the reaction mixture was kept cooled in a salt ice slurry to favour the

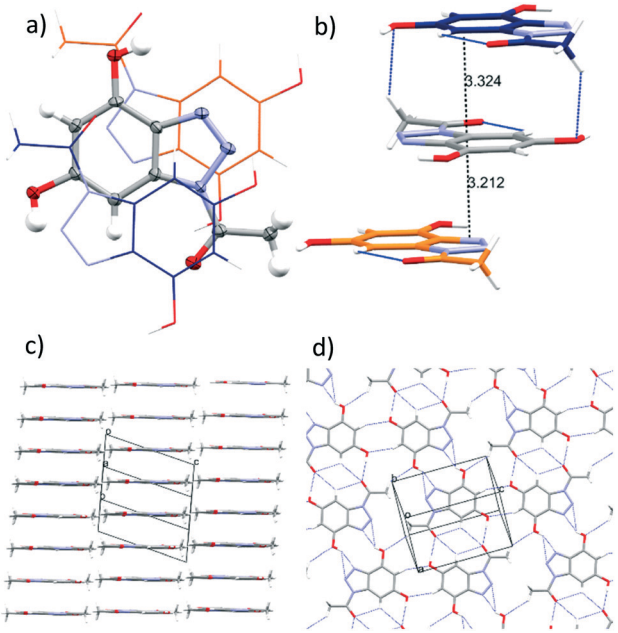

Fig. 4 X-ray crystal structure of dihydroxybenzotriazole **9**, hydrogen bonds are displayed as blue dotted lines; a) overlap in asymmetrical stacked neighbors with hydrogen bonding pair (blue) and lone pair–π interacting pair (orange), ellipsoids are shown at 50% probability; b) side view of asymmetrical anti-parallel continuous stacking; c) 2D sheet formation; d) top-down view of single 2D sheet.

N-formyl product **10** over the *N*-acetyl product **1**. Secondly, treatment of parent benzotriazole **6** with triphosgene under basic conditions followed by quenching with methanol afforded the methyl ester derivative **11**. Lastly, chloroacetyl derivative **12** was obtained by the addition of 2-chloroacetyl chloride to a solution of parent benzotriazole **6** in anhydrous acetone (Scheme 2). The single crystal structure for each of these compounds was subsequently analyzed and relevant data are summarized in Table 1.

Although still forming 2D sheets, parent benzotriazole **6** showed a complete loss of continuous cofacial stacking (Fig. 3a and c). In fact, the only observed π-interactions were between slightly offset dimethoxybenzene rings, which appeared to be stabilized by carbon–hydrogen bonds between the 4-methoxy group of each molecule and occurred over a slightly larger distance of 3.373 ± 0.004 Å. Further diverging from activated benzotriazole **1**, this interaction was non-continuous as it was not present on the opposite face, instead forming a CH–π bond with a 6-methoxy substituent resulting in an interplanar distance of 3.410 ± 0.002 Å (Fig. 3b). This resulted in a packing arrangement more akin to brick-work stacking.[60] The 2D sheets lacked the lattice of carbon–hydrogen bonds, but were rather observed to contain distinct methoxy and triazole domains (Fig. 3d). No short contacts were observed within the methoxy domain, indicating that this arrangement was most likely due to steric effects. It was clear from this crystal structure that the triazole ring–benzene ring stacking in activated benzotriazole **1** was not simply due to a tendency for mixed interactions between heterocyclic and non-heterocyclic rings, but rather required the acetyl group. This also showed that the polarization of N1 by N2 and N3 alone was not enough to elicit donor–acceptor stacking.

Almost antithetical to the packing of parent benzotriazole **6**, *N*-acetylbenzotriazole **8** lacked 2D sheet formation yet still showed continuous stacking at a perpendicular distance of 3.326 ± 0.001 Å (Fig. 3f and h). The packing was also quite distinct from that of activated benzotriazole **1**, exhibiting a parallel orientation with minimal ring overlap that resulted in a herringbone packing mode (Fig. 3e and g). Additionally, this overlap occurred with N3 rather than N1, possibly due to a now relatively electron-deficient benzene ring interacting favorably with the electron rich heterocyclic atom. However, it should be noted that this positioning allowed a substituent–substituent carbon hydrogen bonding between acetyl groups (Fig. 3f). Although it could not be determined which was the driving force in the stacking, it was apparent that the removal of the electron donating group had drastically decreased ring overlap. In combination with the results of parent benzotriazole **6**, it was exceedingly clear that only through a combination of the electron donating methoxy and electron withdrawing acetyl substituents could the donor–acceptor stacking of activated benzotriazole **1** be observed. These results also demonstrated that formation of 2D sheets did not tolerate the removal of the two methoxy substituents.

Demethylation of the methoxy groups to give dihydroxybenzotriazole **9** resulted in a very similar crystal structure to that of activated benzotriazole **1**. This compound gave continuous anti-parallel stacking and likewise formed 2D sheets, however these were found not to be perfectly flat with the aromatic rings lying slightly out of plane by approximately one degree (Fig. 4c). The stacking was also observed to be closer to slipped stacking than cofacial.[60] Peculiarly, this slipped stacking was observed to be asymmetrical on either face of each molecule. On one face, the two molecules were aligned in a very similar manner to the donor–acceptor stacking observed for activated benzotriazole **1** with an almost identical perpendicular stacking distance of 3.324 ± 0.003 Å (Fig. 4a and b in blue). However, the rings were almost completely offset with N1 and its acetyl substituent only just overlapping with the benzene ring. Although the substituent–aromatic interaction with N3 was no longer present, the 6-hydroxy group acted now as a hydrogen bond acceptor, forming a carbon–hydrogen bond with the acetyl substituent of the neighbouring molecule. These results indicated that the substituent-ring interplanar carbon–hydrogen bond of activated benzotriazole **1** was non-essential for the aromatic donor–acceptor stacking between the triazole and benzene ring. On the opposite face, the anti-parallel interaction occurred in a considerably different manner. The two molecules overlapped one another by a far greater extent over a much shorter distance of 3.212 ± 0.002 Å (Fig. 4a and b in orange). This position resulted in the acetyl group undergoing a substituent–substituent π–lone pair interaction with the 4-hydroxy group of the adjacent molecule.

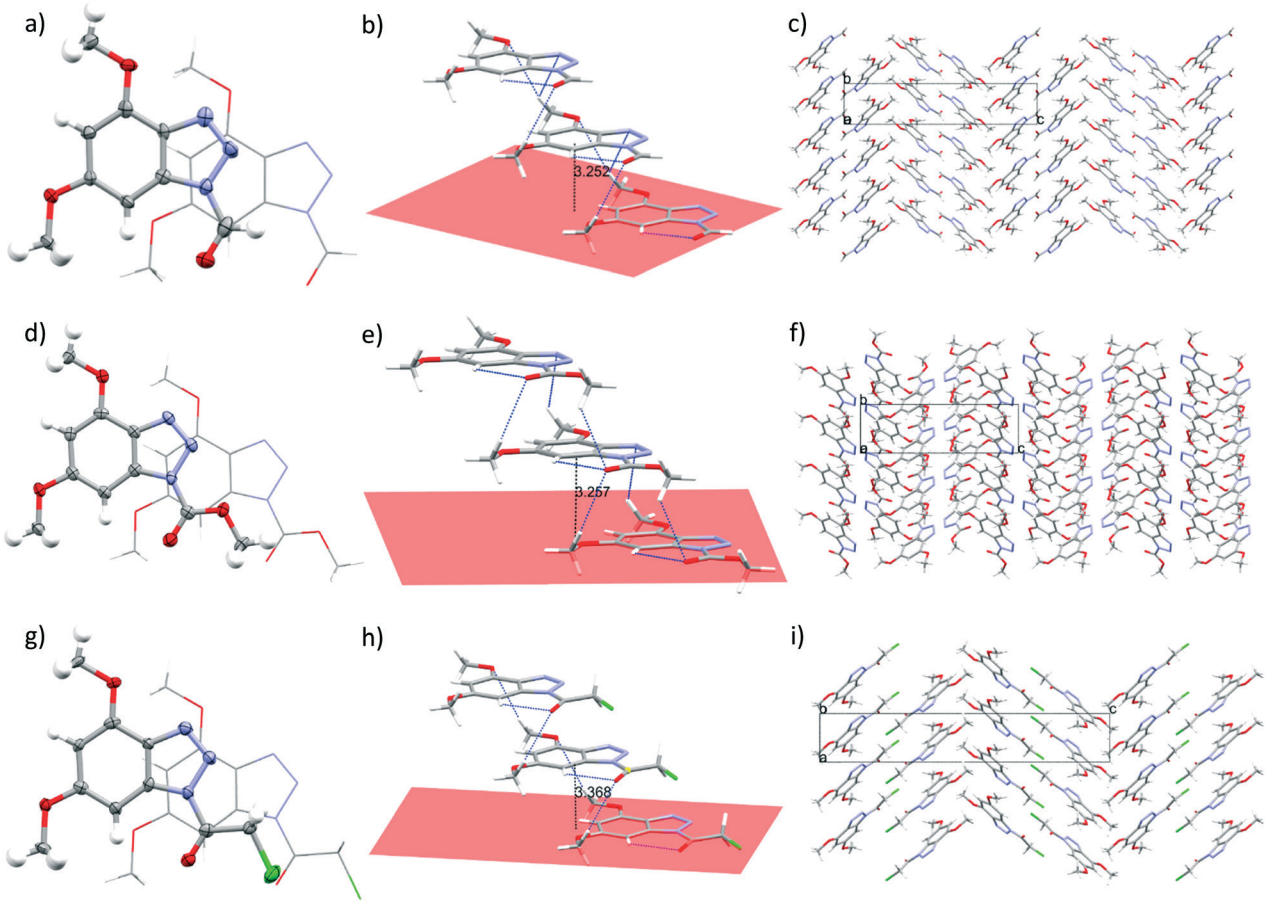

Fig. 5 X-ray crystal structures of formyl derivative **10** (a–c), methyl ester derivative **11** (d–f) and chloroacetyl derivative **12** (g–i); a, d and g) overlap between head–tail stacked molecules, ellipsoids are shown at 50% probability; b, e and h) continuous parallel stacking with hydrogen bonds are displayed as blue dotted lines and plane of bottom molecule in red; c, f and i) herringbone arrays viewed along *b*-axis.

Notably, the 2D sheets formed by dihydroxybenzotriazole **9** contained a network of much stronger conventional OH···O and OH···N hydrogen bonds (Fig. 4d). Although introducing a small amount of torsion to the ring systems, this result in combination with that of *N*-acetylbenzotriazole **8** showed that possession of hydrogen bond accepting oxygens on the benzene ring was crucial to 2D sheet formation.

The single crystal structures of all three N1-substituent analogues **10–12** showed continuous parallel aligned stacking in a herringbone array similar to unactivated benzotriazole **8** (Fig. 5). However, they each differed from the unsubstituted benzotriazole in that they all showed significantly more ring overlap in a donor–acceptor fashion. This overlap was in a similar manner to that of activated benzotriazole **1**, involving both N1 and the α-carbon of each acyl substituent. Whilst donor–acceptor stacking was maintained by the three N1-substituent analogues **10–12**, it was clear that changing the electron withdrawing character of the N1 substituent had little effect on the degree of cofacial overlap. This may have been due to direct substituent interactions, such as the carbon hydrogen bond between the 6-methoxy and *N*-acyl groups in all three structures (Fig. 5b, e and f), or due to other contributing forces to crystal growth. Although the formyl derivative **10** and methyl ester derivative **11** both showed short perpendicular stacking distances of 3.283 ± 0.004 Å and 3.292 ± 0.003 Å respectively, chloroacetyl derivative **12** displayed a larger perpendicular distance of 3.352 ± 0.009 Å. However, this was likely due simply to steric effects from the increased bulk of the chlorine atom.

Due to their similarity in structure to activated benzotriazole **1** it was particularly surprising that none of the three analogues exhibited 2D sheet formation. This result therefore demonstrated the fine-tuned balance achieved by benzotriazole **1** between both electrostatic character and hydrogen bonding capability to exhibit the cofacial stacking that leads to perfectly flat sheets.

Conclusions

In conclusion, the notable crystal packing structure of activated benzotriazole **1** with completely flat sheet formation and antiparallel cofacial stacking was found to be extremely uncommon among benzotriazoles. Furthermore, the unique solid-state assembly has revealed the *N*-acetyl-4,6-dimethoxy-1*H*-benzo[1,2,3]triazole scaffold to be a highly novel aromatic donor–acceptor stacking system that provides both electron rich and

electron deficient areas on a simple bicyclic ring structure. By studying the solid-state assembly of its analogues, we have observed that the electron deficient portions of the triazole ring and acyl substituent associate with a relatively electron rich benzene ring under a variety of substituent conditions. However, this donor–acceptor stacking only occurred with the presence of both electron donating and electron withdrawing groups substituted onto the ring system. Although the interaction was still observed with the use of different electron-donating and electron-withdrawing groups, cofacial stacking was lost in all examples. Similarly, 2D sheet formation was found to be lost with either removal of benzene substituents or modification of the *N*-acyl group. Overall, these results emphasise that the cofacial stacking assembly of activated benzotriazole **1** is extremely sensitive and have been achieved by the molecule only through a sensitive balance of both electrostatic and hydrogen bonding character. Moreover, the observation of substituent–substituent and substituent–aromatic interactions in the cofacially π-stacked molecule is in agreement with the direct substituent model for π-interactions.

Conflicts of interest

There are no conflicts to declare.

Acknowledgements

This work was supported by a Project Grant from the National Health and Medical Research Council (NHMRC) Australia to N. K. [NHMRC Grant APP1008014]. We are thankful to the Nuclear Magnetic Resonance Facility and the Bioanalytical Mass Spectrometry Facility (BMSF) in the Mark Wainwright Analytical Centre at UNSW Sydney for the opportunity of using their instruments.

References

1 S. Hans-Jörg, *Angew. Chem., Int. Ed.*, 2009, **48**, 3924–3977.
2 E. A. Meyer, R. K. Castellano and F. Diederich, *Angew. Chem., Int. Ed.*, 2003, **42**, 1210–1250.
3 D. B. Amabilino and J. F. Stoddart, *Chem. Rev.*, 1995, **95**, 2725–2828.
4 J. Šponer, K. E. Riley and P. Hobza, *Phys. Chem. Chem. Phys.*, 2008, **10**, 2595–2610.
5 J. Šponer, P. Jurečka, I. Marchan, F. J. Luque, M. Orozco and P. Hobza, *Chem. – Eur. J.*, 2006, **12**, 2854–2865.
6 C. A. Hunter, *J. Mol. Biol.*, 1993, **230**, 1025–1054.
7 C. A. Hunter and J. K. Sanders, *J. Am. Chem. Soc.*, 1990, **112**, 5525–5534.
8 J. H. Williams, J. K. Cockcroft and A. N. Fitch, *Angew. Chem., Int. Ed. Engl.*, 1992, **31**, 1655–1657.
9 C. R. Martinez and B. L. Iverson, *Chem. Sci.*, 2012, **3**, 2191–2201.
10 M. J. Rashkin and M. L. Waters, *J. Am. Chem. Soc.*, 2002, **124**, 1860–1861.
11 S. E. Snyder, B. S. Huang, Y. W. Chu, H. S. Lin and J. R. Carey, *Chem. – Eur. J.*, 2012, **18**, 12663–12671.
12 S. E. Wheeler and K. Houk, *J. Am. Chem. Soc.*, 2008, **130**, 10854–10855.
13 S. E. Wheeler, *J. Am. Chem. Soc.*, 2011, **133**, 10262–10274.
14 A. L. Ringer, M. O. Sinnokrot, R. P. Lively and C. D. Sherrill, *Chem. – Eur. J.*, 2006, **12**, 3821–3828.
15 E. C. Lee, D. Kim, P. Jurečka, P. Tarakeshwar, P. Hobza and K. S. Kim, *J. Phys. Chem. A*, 2007, **111**, 3446–3457.
16 S. E. Wheeler, A. J. McNeil, P. Müller, T. M. Swager and K. Houk, *J. Am. Chem. Soc.*, 2010, **132**, 3304–3311.
17 H. Y. Au-Yeung, F. B. Cougnon, S. Otto, G. D. Pantoș and J. K. Sanders, *Chem. Sci.*, 2010, **1**, 567–574.
18 F. B. Cougnon, H. Y. Au-Yeung, G. D. Pantos and J. K. Sanders, *J. Am. Chem. Soc.*, 2011, **133**, 3198–3207.
19 G. Kaiser, T. Jarrosson, S. Otto, Y. F. Ng, A. D. Bond and J. K. Sanders, *Angew. Chem.*, 2004, **116**, 1993–1996.
20 D. G. Hamilton, J. E. Davies, L. Prodi and J. K. M. Sanders, *Chem. – Eur. J.*, 1998, **4**, 608–620.
21 H. Y. Au-Yeung, P. Pengo, G. D. Pantos, S. Otto and J. K. M. Sanders, *Chem. Commun.*, 2009, 419–421, DOI: 10.1039/B816979A.
22 A. Das, M. R. Molla, A. Banerjee, A. Paul and S. Ghosh, *Chem. – Eur. J.*, 2011, **17**, 6061–6066.
23 M. R. Molla, A. Das and S. Ghosh, *Chem. – Eur. J.*, 2010, **16**, 10084–10093.
24 V. Percec, M. Glodde, T. Bera, Y. Miura, I. Shiyanovskaya, K. Singer, V. Balagurusamy, P. Heiney, I. Schnell and A. Rapp, *Nature*, 2002, **419**, 384.
25 H. M. Colquhoun, Z. Zhu, D. J. Williams, M. G. Drew, C. J. Cardin, Y. Gan, A. G. Crawford and T. B. Marder, *Chem. – Eur. J.*, 2010, **16**, 907–918.
26 A. Marcos Ramos, S. C. Meskers, E. H. Beckers, R. B. Prince, L. Brunsveld and R. A. Janssen, *J. Am. Chem. Soc.*, 2004, **126**, 9630–9644.
27 S. Burattini, H. M. Colquhoun, J. D. Fox, D. Friedmann, B. W. Greenland, P. J. Harris, W. Hayes, M. E. Mackay and S. J. Rowan, *Chem. Commun.*, 2009, 6717–6719.
28 S. Burattini, B. W. Greenland, D. H. Merino, W. Weng, J. Seppala, H. M. Colquhoun, W. Hayes, M. E. Mackay, I. W. Hamley and S. J. Rowan, *J. Am. Chem. Soc.*, 2010, **132**, 12051–12058.
29 H. M. Colquhoun, D. J. Williams and Z. Zhu, *J. Am. Chem. Soc.*, 2002, **124**, 13346–13347.
30 J. C. Barnes, M. Juríček, N. L. Strutt, M. Frasconi, S. Sampath, M. A. Giesener, P. L. McGrier, C. J. Bruns, C. L. Stern, A. A. Sarjeant and J. F. Stoddart, *J. Am. Chem. Soc.*, 2013, **135**, 183–192.
31 L. Chen, Y.-M. Zhang, L.-H. Wang and Y. Liu, *J. Org. Chem.*, 2013, **78**, 5357–5363.
32 H. M. Colquhoun, Z. Zhu and D. J. Williams, *Org. Lett.*, 2003, **5**, 4353–4356.
33 T. Uchikura, K. Ono, K. Takahashi and N. Iwasawa, *Angew. Chem., Int. Ed.*, 2018, **57**, 2130–2133.
34 C. G. Claessens and J. F. Stoddart, *J. Phys. Org. Chem.*, 1997, **10**, 254–272.
35 S. A. Nepogodiev and J. F. Stoddart, *Chem. Rev.*, 1998, **98**, 1959–1976.

36 L. Fang, S. Basu, C.-H. Sue, A. C. Fahrenbach and J. F. Stoddart, *J. Am. Chem. Soc.*, 2010, **133**, 396–399.
37 C. J. Bruns, J. Li, M. Frasconi, S. T. Schneebeli, J. Iehl, H. P. Jacquot de Rouville, S. I. Stupp, G. A. Voth and J. F. Stoddart, *Angew. Chem., Int. Ed.*, 2014, **53**, 1953–1958.
38 S. K. Dey, A. Coskun, A. C. Fahrenbach, G. Barin, A. N. Basuray, A. Trabolsi, Y. Y. Botros and J. F. Stoddart, *Chem. Sci.*, 2011, **2**, 1046–1053.
39 T. Iijima, S. A. Vignon, H. R. Tseng, T. Jarrosson, J. K. Sanders, F. Marchioni, M. Venturi, E. Apostoli, V. Balzani and J. F. Stoddart, *Chem. – Eur. J.*, 2004, **10**, 6375–6392.
40 R. S. Lokey and B. L. Iverson, *Nature*, 1995, **375**, 303.
41 C. Peebles, R. Piland and B. L. Iverson, *Chem. – Eur. J.*, 2013, **19**, 11598–11602.
42 J. J. Reczek and B. L. Iverson, *Macromolecules*, 2006, **39**, 5601–5603.
43 B. A. Ikkanda, S. A. Samuel and B. L. Iverson, *J. Org. Chem.*, 2014, **79**, 2029–2037.
44 P. M. Alvey, J. J. Reczek, V. Lynch and B. L. Iverson, *J. Org. Chem.*, 2010, **75**, 7682–7690.
45 J. J. Reczek, K. R. Villazor, V. Lynch, T. M. Swager and B. L. Iverson, *J. Am. Chem. Soc.*, 2006, **128**, 7995–8002.
46 D. G. Hamilton, D. E. Lynch, K. A. Byriel, C. H. L. Kennard and J. K. M. Sanders, *Aust. J. Chem.*, 1998, **51**, 441–444.
47 M. Wang and F. Wudl, *J. Mater. Chem.*, 2012, **22**, 24297–24314.
48 L. F. Dössel, V. Kamm, I. A. Howard, F. D. R. Laquai, W. Pisula, X. Feng, C. Li, M. Takase, T. Kudernac and S. De Feyter, *J. Am. Chem. Soc.*, 2012, **134**, 5876–5886.
49 C. Peebles, P. M. Alvey, V. Lynch and B. L. Iverson, *Cryst. Growth Des.*, 2013, **14**, 290–299.
50 T. L. Benanti, P. Saejueng and D. Venkataraman, *Chem. Commun.*, 2007, 692–694.
51 K. Kobayashi, R. Shimaoka, M. Kawahata, M. Yamanaka and K. Yamaguchi, *Org. Lett.*, 2006, **8**, 2385–2388.
52 M. D. Curtis, J. Cao and J. W. Kampf, *J. Am. Chem. Soc.*, 2004, **126**, 4318–4328.
53 K. Pchalek, A. W. Jones, M. M. Wekking and D. StC. Black, *Tetrahedron*, 2005, **61**, 77–82.
54 P. A. Keller, N. Kumar and D. StC. Black, *Tetrahedron*, 2008, **64**, 11603–11610.
55 G. B. McGaughey, M. Gagné and A. K. Rappé, *J. Biol. Chem.*, 1998, **273**, 15458–15463.
56 J. Singh, R. Fox, M. Wong, T. P. Kissick, J. L. Moniot, J. Z. Gougoutas, M. F. Malley and O. Kocy, *J. Org. Chem.*, 1988, **53**, 205–208.
57 G. Boche, P. Andrews, K. Harms, M. Marsch, K. S. Rangappa, M. Schimeczek and C. Willeke, *J. Am. Chem. Soc.*, 1996, **118**, 4925–4930.
58 C. Janiak, *J. Chem. Soc., Dalton Trans.*, 2000, 3885–3896.
59 A. E. Pasqua, M. Matheson, A. L. Sewell and R. Marquez, *Org. Process Res. Dev.*, 2011, **15**, 467–470.
60 M. Mas-Torrent and C. Rovira, *Chem. Rev.*, 2011, **111**, 4833–4856.

